*Lasers in Eng.*, Vol. 56, pp. 209–224
Reprints available directly from the publisher
Photocopying permitted by license only



# Wet Laser Cleaning of Paint Layers from the Surface of a Carbon Fibre Reinforced Polymer (CFRP)

H-X. LIU[1,2,*], W-F. PAN[1,2], X. CHEN[1,2], M-J. CHEN[1,2], Z-J. ZHAO[1,2], L. LIU[1,2] AND F. SONG[1.2,*]

[1]*The Key Laboratory of Weak Light Nonlinear Photonics (Ministry of Education), School of Physics, Nankai University, 94 Weijin Road, Tianjin 300071, China*
[2]*Collaborative Innovation Center of Extreme Optics, Shanxi University, 92 Wucheng Road, Xiaodian, Taiyuan 030006, Shanxi Province, China*

By monitoring the surface temperature of a carbon fibre reinforced polymer (CFRP) sample, we designed a wet laser cleaning method to successfully remove the paint and surface epoxy resin layer without damaging the CFRP substrate. The temperature and stress distributions at the interface between the epoxy resin and CFRP were simulated by the heat conduction equation. The variation trend of temperature and stress with the average laser power was obtained and the cleaning threshold was given. A 1064 nm acoustic-optical Q-switched laser was used for cleaning by scanning the painted CFRP sample at a certain speed with different laser powers and the cleaning effect was monitored by measuring the temperature in real-time. The cleaning mechanism in the wet laser cleaning of CFRP is indicated to be the thermal stress stripping mechanism.

*Keywords: Fibre laser, carbon fibre reinforced polymer (CFRP), wet laser cleaning, paint removal, thermal stress, simulation, Fluent*

## 1 INTRODUCTION

In recent years, composite materials have been increasingly used in industries such as aerospace and automotive manufacturing due to their higher strength, chemical corrosion resistance and dimensional stability [1]; for example, in

*Corresponding authors: E-mail: liuhanxiong@mail.nankai.edu.cn (H-X. Liu), fsong@nankai.edu.cn (F. Song)

the Boeing 787 and Airbus A350, more than 50% of the total materials are made of composite materials [2].

Carbon fibre reinforced polymer (CFRP) is one of the most widely used resin matrix composite materials [3], which is composed of carbon fibre reinforced material and epoxy resin polymer matrix material. It has the characteristics of corrosion resistance, high strength and low density [4]. Coating paint layers on CFRP surface is a common method for protecting it and marking decoration. In the process of use, the paint layer could be scratched, cracked and oxidized under the influence of temperature, humidity, ultraviolet (UV) and other environmental factors [5], which will affect the strength of the composite material and cause its performance to decline [6]. This requires the removal of the paint layers and respraying of the underlying CFRP periodically.

The composite structure of CFRP is mainly composed of two parts. The first part is a network of carbon fibres [7] whose integrity determines the strength of CFRP. The second part is the epoxy resin structure, including curing epoxy resin and sizing agent. Curing resin is used in the CFRP structure to keep the shape of carbon fibre products and make the surface of CFRP smooth [8]. Sizing agent is used in CFRP manufacturing to ensure the short carbon's stability and make the surface of carbon fibre smooth [7].

The traditional paint removal methods such as sandblasting and chemical treatment, are easy to damage carbon fibres of CFRP. Laser cleaning, as a green, environmentally friendly and selective cleaning method has been used for cleaning various paint layers on different substrates [9] But the carbon fibres are easily damaged in the laser processing as well when the substrate is CFRP [10]. This is because the curing resin and sizing agent are usually epoxy resin with low curing temperature, low curing shrinkage ratio and relatively low thermal decomposition temperature. The thermal decomposition temperatures of them are usually lower than that of polyurethane paint [11]. Sizing agent is easy to be decomposed so that the carbon fibre disintegrates to short fibres and burr shape appears on the CFRP surface during the laser process [12, 13]. If the decomposition of sizing agent happens, it is hard to be repaired; however, the curing resin is easy to be repaired by secondary curing with liquid resin [14, 15]. As such, when using laser to remove CFRP surface coating, the loss of resin is acceptable while the disintegrating of carbon fibres should be avoided.

Few research has been reported on laser cleaning of paint from CFRP due to the difficulty to avoid the damage of the substrate [16]. Yang *et al.* [17] studied the pulsed laser parameters in the case of incomplete removal of paint layers on the surface of CFRP composites. The effect of laser scanning speed in the cleaning of CFRP by UV light was studied by Gao *et al.* [18]. Genna *et al.* [16] studied the change of CFRP intensity after using laser cleaning of CFRP. Lu *et al.* [19] simulated the generation of plasma and the effect of nanosecond laser cleaning paint on the surface of CFRPs. The CFRP related

repair techniques were summarized in a review by Katnam *et al.* [20]. Based on these studies, this paper is working on the wet laser cleaning to remove the paint completely with no damage caused to the CFRPs.

The two main mechanisms of laser cleaning are ablation mechanism and thermal stress mechanism [21, 22]. For the ablation mechanism, the paint absorbs laser heat to reach its thermal decomposition temperature or vaporization temperature, thereby achieving the purpose of paint removal [23-25]; however, it is extremely difficult to carefully adjust the laser parameters so that the laser energy can be absorbed only by the paint layer. For the high decomposition temperature of the paint layer, sizing agent has easily been decomposed with the paint layer is removed. In the thermal stress mechanism, when the thermal stress caused by the laser is greater than the binding force, the paint layer and the substrate can be peeled off [26]. In this process, the paint and the substrate do not need to reach the thermal decomposition temperature, so as to better protect the substrate.

In order to remove the CFRP surface paint while avoiding damage to the CFRP substrate, we developed a wet laser cleaning method, using thermal stress mechanism, to peel the paint layer from the CFRP surface at a lower temperature, which is put forward the first time to our best knowledge. In this paper, the thermal stress curve of CFRP was obtained by simulation, and then verified by experiments in wet laser cleaning. The results show that the paint on the surface of CFRP can be better removed without damaging the carbon fibres by selecting appropriate parameters of laser. In order to ensure the cleaning effect and avoid the damage of CFRP, we monitored the cleaning situation in real-time by means of temperature measurement.

## 2 EXPERIMENTAL DETAILS

### 2.1 Materials and sample preparation techniques

The sample used in the experiment was a T300 CFRP (Hengshen Company Ltd.), obtained as a square of $30 \times 30$ cm$^2$ with a thickness of 2 mm. The paint used was orange polyurethane paint (Baijia Company Ltd.), sprayed onto the CFRP substrate to a thickness of 0.5 mm. Figure 1 shows the CFRP sample in its bare state, in its painted state and the structure diagram after spray painting. The thermo-physical properties of CFRP and paint are given in Table 1. Several identical samples were made for testing and experimentation. Carbon fibre pre-woven fabric is orthogonal braided.

The epoxy resin and the polyurethane paint in/on the CFRP were subjected to thermogravimetric analysis (TGA). The TGA curves obtained are shown in Figure 2 where it can be seen that the thermal decomposition of the epoxy resin begins at 100ºC, much lower than that of paint at 200ºC. The thermal decomposition process of the epoxy resin and paint basically end at 400ºC; therefore, if the ablative mechanism is used to remove the paint, the


FIGURE 1
(a) Photograph of the bare CFRP, (b) photograph of the painted CFRP and (c) section drawing of painted CFRP sample.

TABLE 1
Thermo-physical properties of the materials used in this work.

| Property | T300 Carbon Fibre | Epoxy Resin | Polyurethane Paint |
|---|---|---|---|
| Density (kg/cm$^3$) | 1760 | 1200 | 2000 |
| Young's modulus (Pa) | $2.3 \times 10^{11}$ | $1.0 \times 10^{9}$ | $2.0 \times 10^{8}$ |
| Specific heat capacity (J/kgK) | 795 | 550 | 560 |
| Heat conductivity (W/mK) | 10.5 | 2.0 | 0.2 |
| Coefficient of thermal expansion (1/K) | $5.00 \times 10^{-7}$ | $5.68 \times 10^{-5}$ | $1.80 \times 10^{-4}$ |

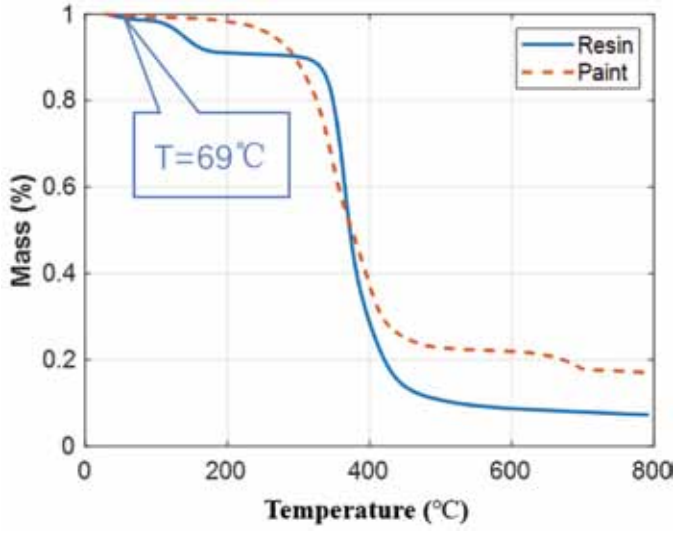


FIGURE 2
The TGA curves of the epoxy resin and the paint.

laser beam needs only to be absorbed by the paint layer without heat transfer to the CFRP substrate, which is difficult to control and realize. This then leaves the thermal stress mechanism as the appropriate ablative mechanism. This was achieved by preventing the temperature from rising too fast by placing a sample in a tank with a height of 2 mm from the surface of the water. The water flowed at a certain speed, taking the heat away.

### 2.2 Paint removal apparatus and processing procedures

A laser system (Institute of Semiconductor of Chinese Academy of Sciences) emitting a Gaussian beam at a wavelength of 1064 nm with a maximum average output power of 500 W, repetition frequency of 20 kHz and pulse width of 100 ns was used. A galvanometer and guide rail (GR200; Lubang Ltd.) were used to control the laser beam path. The scanning speed of the galvanometer used in the system was 2 m/s. By using a moving guide rail the translation running speed was kept constant at 0.6 m/s with an overlap rate of 0. The laser spot was a circle with a diameter of 1 mm. The system configuration is shown in Figure 3 and the scanning path of laser beam is shown in Figure 4. The. The laser cleaning efficiency in this scanning mode was the highest and did not cause damage to the carbon fibres. Six laser powers ranging from 50 to 100 W were used for the paint removal. The maximum temperature of the paint layer surface was recorded with a temperature detector (H13; HIKMICRO Ltd.).

### 2.3 Sample analysis techniques

The binding force was be measured using a standard sample prepared in accordance with ASTM D5868-2001. Therein the CFRP surface epoxy resin

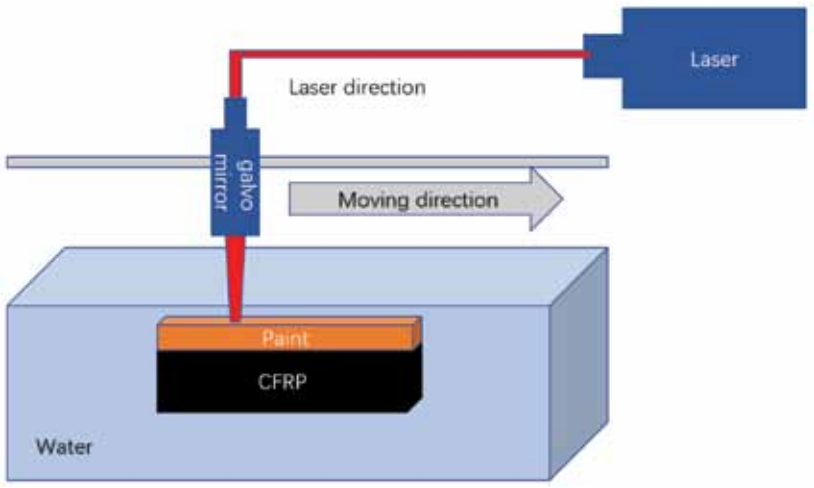


FIGURE 3
Schematic diagram of laser cleaning system.

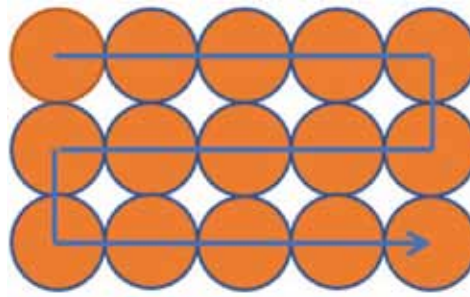

FIGURE 4
The scanning path of laser. The circle represents the laser transitional beam profile.

was removed and then bonded with epoxy resin. The tensile strength was tested with a tensile testing machine (LGD5000; Lu Gong Ltd.) and the average value of three testing runs was taken as the binding force between the surface epoxy resin and carbon fibre.

The laser paint removal performance was imaged using a camera (EOS 850D; Canon Ltd.). To further analyse the laser paint removal performance CFRP were observed with a scanning electron microscope (SEM) fitted with an energy dispersive spectroscope (EDS) (JMS-7500F; JEOL Ltd.).

## 3 MODEL DEVELOPMENT AND ASSESSMENT

### 3.1 Build and assumptions

The heat transfer model is shown in Figure 5. The laser beam acts on the surface of the paint layer. The paint layer absorbs the heat and transfer the heat downward. The surface epoxy resin and carbon fibre expansion with the temperature increasing. When the thermal stress generated by thermal expansion is greater than the binding force between carbon fibre and the surface epoxy resin layer, fracture occurs and the paint layer peels off.

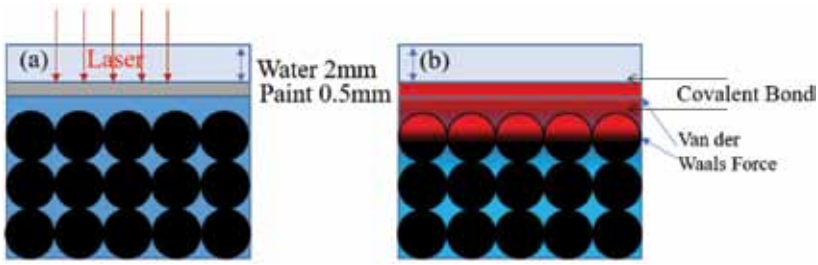


FIGURE 5
Schematic diagram of the heat transfer model.

The heat transfer process between paint layer, the CFRP substrate and water layer satisfies the heat conduction equation [27]

$$\frac{\partial}{\partial t}(\rho E)+\nabla\left(\vec{v}(\rho E+P)\right)=\nabla\left(K_{eff}\nabla T\right)-\sum_{j}h_{j}\vec{j}_{j}+(\bar{\bar{\tau}}_{eff}\vec{v})+S_{h} \tag{1}$$

with $E$, the energy *per* unit mass, given by

$$E=h-\frac{p}{\rho}+\frac{v^{2}}{2} \tag{2}$$

where $\rho$ is the density of the element, $\vec{v}$ is the speed of the element, $K_{eff}$, is the effective conductivity ($k$+$kf$, where $k$ is the thermal conductivity and $kf$ the turbulent thermal conductivity), $J$ is the diffusion flux of species $j$, $S_h$ includes the heat of chemical reaction and other volumetric heat source, $h$ is the sensible enthalpy and $\bar{\bar{\tau}}_{eff}$ is effective coefficient of viscous dissipation.

The thermal stress, $\sigma$, satisfies the thermal expansion equation [28]:

$$\sigma=Y_{c}\nabla T(a_{c}-a_{s}) \tag{3}$$

where $Y_c$ Young's modulus of the upper contact surface, $\nabla T$ is the temperature gradient, $a_c$ is the first element of the upper contact surface and $a_s$ the second element of the lower contact surface.

The laser intensity on the surface of the paint layer, $I$, is given by

$$I(x,z,t)=\frac{2P}{\pi * r^{2}}\exp\left\{-\frac{2\left[\left(x-v*t\right)+z\right]^{2}}{r^{2}}\right\} \tag{4}$$

where $P$ is the average power of the laser, $r$ the radius of the laser spot and $v$ the speed of laser scanning.

The water inlet temperature is room temperature (300 K) and the water flow rate is 1 m/s; consequently, the boundary can be considered as a constant temperature boundary of 300 K.

According to the sample structure, the equivalent model was established by the requirements of Fluent for mesh. The equivalent model had two layers of carbon fibre mesh, each layer of carbon fibre mesh was arranged horizon-

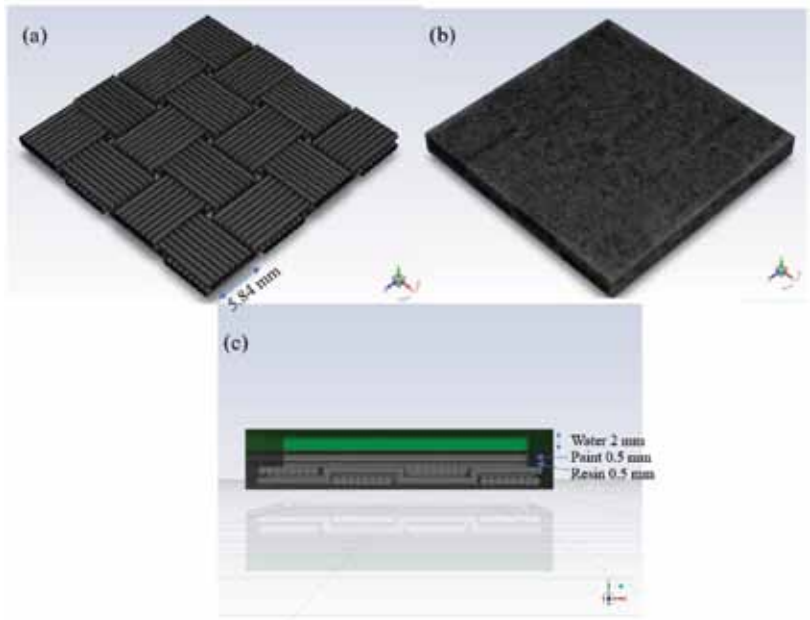


FIGURE 6
Rendered images of (a) the carbon fibre grid pattern, (b) upper surface of the model and (c) cross-section of the model.

tally and vertically. The diameter of carbon fibre was 0.8 mm, the superposition rate of 10% was adopted. Each eight carbon fibres were formed into a group. The carbon fibre was covered with a 0.5 mm thick surface epoxy resin layer. A 0.5 mm thick paint layer was added on the surface of the epoxy resin layer, and a 2 mm thick flowing water layer was covered on the paint layer to simulate the environmental requirements of wet cleaning. The grid is shown in Figure 6. Fluent software was used to simulate the temperature field and thermal stress distribution of the model, as well as the relationship between laser power and thermal stress.

### 3.2 Distribution of temperature field and thermal stress

The results of temperature field and thermal stress are shown in Figure 7. The material parameters used in the simulation are given in Table 1. As can be seen from Figure 7(a), due to the thermal conductivities of materials are relatively low, the high temperature area mainly located on the surface of the paint layer and had little influence on the CFRP. It can be seen from Figure 7(b) that the high thermal stress area is mainly concentrated on the contact interface of surface CFRP and surface epoxy resin with the highest thermal stress of $5.13 \times 10^7$ Pa. It can be seen from Figure 7 that the region of thermal stress is larger than that of the laser action, which is caused by

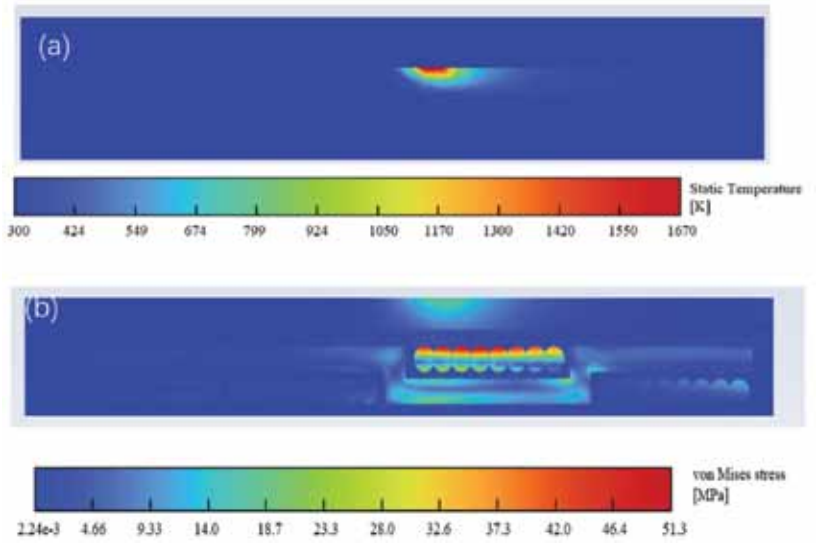


FIGURE 7
Simulation results showing (a) the temperature field distribution and (b) the thermal stress distribution.

thermal diffusion. The thermal stress mainly affects the surface CFRP but has little effect on the lower CFRP.

### 3.3 Influence of laser power on thermal stress

In order to further investigate the variation trend we used different laser powers to simulate. The temperature distribution and thermal stress distribution were calculated when the average laser power was 60 to 120 W. The maximum surface temperatures and maximum thermal stresses of CFRP under different laser powers are shown in Figure 8.

As can be seen from Figure 8, the surface temperature and thermal stress of CFRP increase with the increasing of laser power. Because the laser only acts on the surface of the paint layer, the thermal conductivity between the paint layer and the epoxy resin is small and the laser pulse width is very short, it is difficult to complete the heat exchange between the water layer and the surface of the epoxy resin layer during the duration of one pulse. Under the action of multiple laser pulses, the maximum temperature increases faster than the laser power with the heat accumulation. The thermal stress increases fast with the increasing of temperature. Cleaning is completed when the thermal stress is greater than the binding force between the surface CFRP and the surface epoxy resin.

The tensile strength was measured as 16.76, 17.60 and 19.41 MPa, and the binding force between surface epoxy resin and surface of the CFRP was measured to be 17.92 MPa as an average. According to the data in Figure 8, when

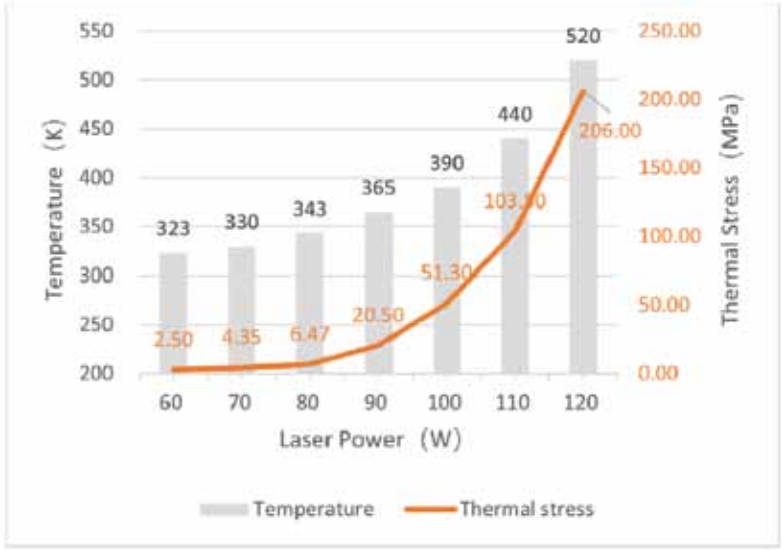


FIGURE 8
Graph showing the maximum temperature and thermal stress in the CFRP surface at different powers.

the laser power exceeds 90 W the thermal stress is greater than the binding force and thus the paint removal can be completed, with 90 W being the threshold laser power.

## 4 RESULTS AND DISCUSSION

### 4.1 General experimental observations

With the laser scanning on the sample, the surface bulge appeared on the surface of paint layer, as shown in Figure 9. When the bulge reaches a certain degree the paint layer can be easily peeled off from the CFRP surface by using a high pressure water gun. In the whole laser paint removal process, there was no ablation phenomenon and the paint layer was intact and did not rupture, showing that the main cleaning mechanism was thermal stress rather than thermal ablation.

The laser paint removal results obtained with different powers are shown in Figure 10. When the laser power was 50 W, there was no obvious change on the sample surface. When the laser power was 60 W, peeling occurred; when the laser power increased to 70 W, the phenomenon of paint peeling from the CFRP substrate surface was obvious, which could be considered as the laser paint removal threshold. When the laser power increased to 80 and 90 W, the thermal stress generated by the laser was greater than the bonding

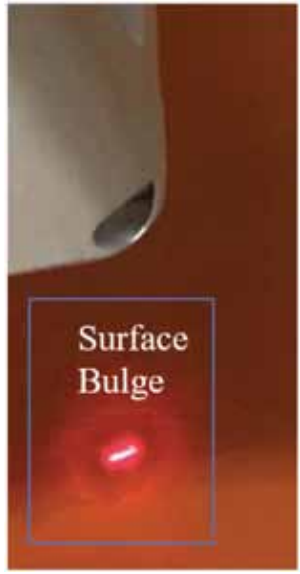


FIGURE 9
Photograph showing the surface bulge observed in the paint layer following laser scanning.

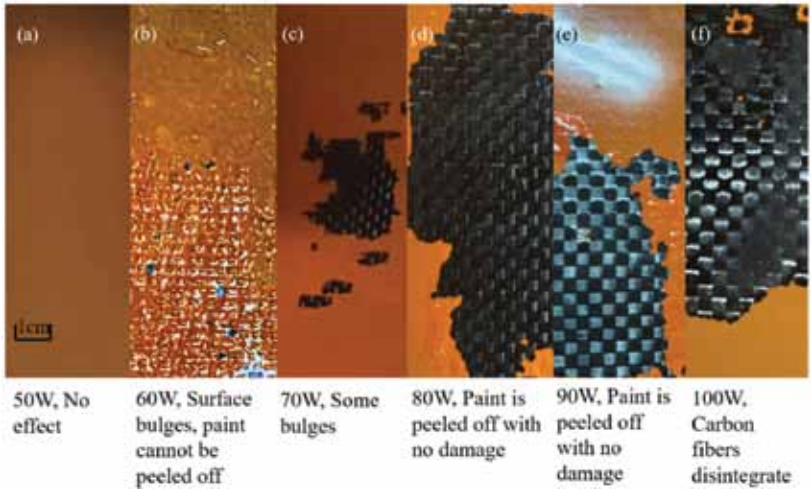


FIGURE 10
Results obtained with different laser powers.

force between the CFRP and the surface epoxy resin layer, and the paint layer peeled off besides the edge area of CFRP sample. There was no damage to the carbon fibres; furthermore, the thermal decomposition of sizing agent

happened at the centre of the laser spot when the laser power increased to 100 W. The short fibre contained in the CFRP displayed burrs on the surface of the CFRP for lacking the binding of the sizing agent.

The laser paint removal effect is shown in Figure 11, where it can be seen from Figure 11(a) that the paint layer forms a foamed surface morphology with laser power of 60 W. In Figure 11(b), the CFRP keeps good while the paint layer peels off with a laser power of 80 W. When the laser power is 90 W it can be seen from Figure 11(c) that the sizing agent begins to decompose, the surface of the CFRP forms a honeycomb structure. This kind of honeycomb adhesive layer wraps a single carbon fibre without binding itself, which indicates that this layer is a carbon fibre surface sizing agent rather than a surface epoxy resin layer in the CFRP. The presence of short fibres can be clearly seen from the sizing agent, but the sizing agent can still maintain the structural stability of the carbon fibre. In Figure 11(d) it can be seen that when the laser power is 100 W, the sizing agent cannot maintain the structural stability of the carbon fibres and the carbon fibres disintegrated into short fibres, which indicated that the CFRP was damaged. It can be seen that most of the broken carbon fibres still maintain the original arrangement direction, and a

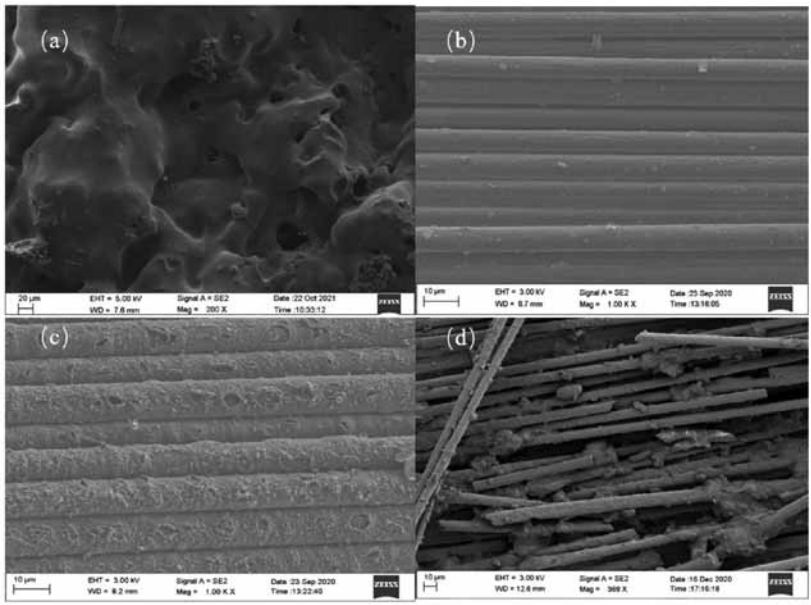


FIGURE 11
SEM micrographs showing (a) the surface pattern on the paint layer obtained with a laser power of 60 W, (b) the undamaged carbon fibres after paint removal with a laser power of 80 W, (c) the surface pattern of the carbon fibres after paint removal with a laser power of 80 W with part of the sizing agent decomposed and (d) the damaged carbon fibre pattern after paint removal with a laser power of 100 W.

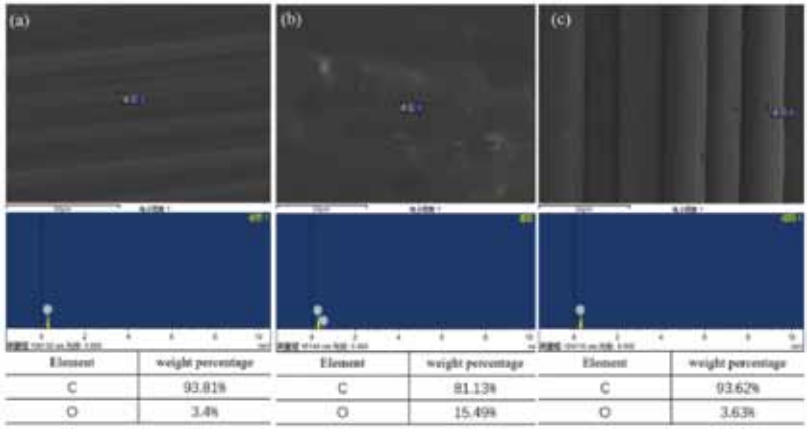


| Element | weight percentage |
|---|---|
| C | 93.81% |
| O | 3.4% |

| Element | weight percentage |
|---|---|
| C | 81.13% |
| O | 15.49% |

| Element | weight percentage |
|---|---|
| C | 93.62% |
| O | 3.63% |

FIGURE 12
EDS spectra and content details of C and $O_2$ for (a) the bare CFRP, (b) the painted CFRP surface and (c) the CFRP surface after laser paint removal.

small amount of broken carbon fibres are transversely stemmed, which is microscopically manifested as the surface morphology of burrs.

From Figure 12 it can be seen that the exposed CFRP has similar $O_2$ content distribution and C content distribution to the original CFRP. After laser paint removal, the $O_2$ content of the CFRP sample surface decreases rapidly and is close to that of the original state. This proves the integrity of the CFRP throughout the wet laser cleaning process.

### 4.2 Real-time temperature monitoring

Figure 13 shows the temperature with different laser powers. When the laser power was 50 W, the laser paint removal has not yet occurred and the temperature is slightly higher than the room temperature of 35.0°C. With laser powers of 60 to 90 W, the temperature is between 37.5 to 45.0°C, while the sizing agent has not decomposed. When the laser power was 100 W, the thermal stress is much greater than the binding force and the excess heat is absorbed by the CFRP. The temperature has a sudden rise to 60.0°C, which means that the sizing agent in the CFRP undergoes thermal decomposition resulting in a rapid increase in temperature; thus, the laser paint removal process can be monitored and controlled by measuring the temperature. The experimental trend of the temperature on laser power is similar to the theoretical simulation shown in Figure 8.

### 4.3 Model-informed findings

According to the simulation results and experimental results the laser paint removal of the CFRP needs to meet two requirements. The first requirement

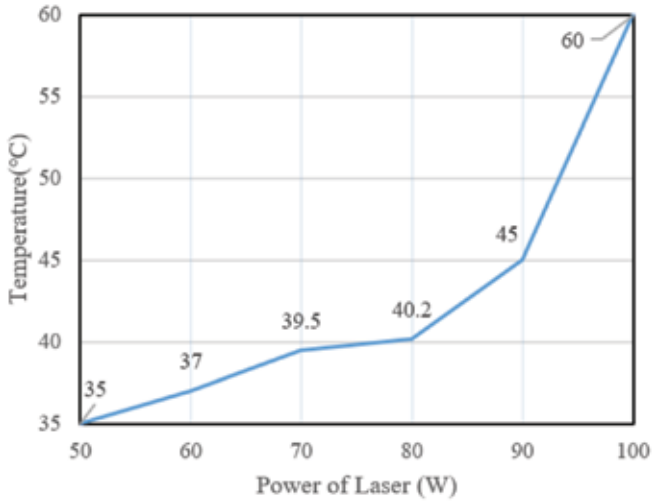


FIGURE 13
Graph showing the maximum surface temperature of the paint layer with different powers.

is that the thermal stress between the surface epoxy resin and the surface carbon fibres which is generated by laser, $F_1$, is greater than the binding force between surface carbon fibres and surface epoxy resin, $F_2$. The second requirement is that the highest temperature of carbon fibres during laser action, $T_1$, is less than the thermal decomposition temperature of sizing agent in carbon fibres, $T_2$. From our work the best laser power to remove the paint layer from the surface of the CFRP was between 80 and 90 W. The specific laser paint removal parameters are determined by various factors such as carbon fibre type, laser energy distribution, paint layer type and thickness.

Thermal stress is affected by both laser power and heat accumulation effect. With the increase of laser power, the thermal stress increases. At the edge of the painted CFRP samples the peeling force between the paint layer and the CFRP substrate is decreased due to the weakening of the heat accumulation effect. The best laser paint removal power threshold by simulation is close to the experimental results.

## 5 CONCLUSIONS

Analytical simulation combined with experiments of removing a paint layer on the surface of a carbon fibre reinforced polymer (CFRP) substrate with a 1064 nm acoustic-optic Q-switched fibre laser was explored as a wet laser cleaning method. The work has solved the thorny problem that the carbon fibres are easy to be damaged. When the scanning speed is 0.6 m/s the most

suitable laser paint removal range is between 80 and 90 W, which can effectively remove the paint layer and protect the underlying CFRP from damage. The theoretical simulation is consistent with the experimental results. By monitoring the maximum temperature of the sample surface in real-time, the damage to the CFRP is effectively avoided and the work efficiency is improved.

## ACKNOWLEDGEMENTS

This work was supported by the National Key Research and Development Program of China (Grant No. 2022YFB4601500).

## REFERENCES

[1] Soutis C. Fibre reinforced composites in aircraft construction. *Progress in Aerospace Sciences* **41**(2) (2005), 143-151.
[2] Xu H., Hu J. and Yu Z. Absorption behavior analysis of carbon fiber reinforced polymer in laser processing. *Optical Materials Express* **5**(10) (2015), 2330-2336.
[3] Xu H. and Hu J. Modeling of the material removal and heat affected zone formation in CFRP short pulsed laser processing. *Applied Mathematical Modelling* **46** (2017),354-364.
[4] Leone C., Genna S. and Tagliaferri V. Fibre laser cutting of CFRP thin sheets by multi-passes scan technique. *Optics and Lasers in Engineering* **53** (2014), 43-50.
[5] Rivas T., Pozo-Antonio J., López de Silanes M., Ramil A. and López A. Laser versus scalpel cleaning of crustose lichens on granite. *Applied Surface Science* **440** (2018), 467-476.
[6] Zhang Z., Shan J., Tan X. and Zhang J. Effect of anodizing pre-treatment on laser joining CFRP to aluminum alloy A6061. *International Journal of Adhesion and Adhesives* **70** (2016), 142-151.
[7] Fischer F., Kreling S. and Dilger K. Surface Structuring of CFRP by using Modern Excimer Laser Sources. *Physics Procedia* **39** (2012), 154-160.
[8] Mandolfino C., Lertora E., Genna S., Leone C. and Gambaro C. Effect of laser and plasma surface cleaning on mechanical properties of adhesive bonded joints. *Procedia CIRP* **33** (2015), 458-463.
[9] Dimogerontakis T., Oltra R. and Heintz O. Thermal oxidation induced during laser cleaning of an aluminium-magnesium alloy. *Applied Physics A:Materials Science & Processing* **81**(6) (2005), 1173-1179.
[10] Sorrentino L., Marfia S., Parodo G. and Sacco E. Laser treatment surface: An innovative method to increase the adhesive bonding of ENF joints in CFRP. *Composite Structures* **233** (2020).
[11] Leone C., Papa I., Tagliaferri F. and Lopresto V. Investigation of CFRP laser milling using a 30W Q-switched Yb:YAG fiber laser: Effect of process parameters on removal mechanisms and HAZ formation. *Composites Part A: Applied Science and Manufacturing* **55** (2013), 129-142.
[12] Oliveira V., Sharma S., de Moura M., Moreira R. and Vilar R. Surface treatment of CFRP composites using femtosecond laser radiation. *Optics and Lasers in Engineering* **94** (2017), 37-43.
[13] Weber R., Hafner M., Michalowski A. and Graf T. Minimum damage in CFRP laser processing. *Physics Procedia* **12** (2011), 302-307.
[14] Fischer F., Romoli L. and Kling R. Laser-based repair of carbon fiber reinforced plastics. *CIRP Annals* **59**(1) (2010), 203-307.

[15] Caminero M., Pavlopoulou S., Lopez-Pedrosa M., Nicolaisson B., Pinna C. and Soutis C. Analysis of adhesively bonded repairs in composites: Damage detection and prognosis. *Composite Structures* **95** (2013), 500-517.

[16] Genna S., Lambiase F. and Leone C. Effect of laser cleaning in laser assisted joining of CFRP and PC sheets. *Composites Part B: Engineering* **145** (2018), 206-214.

[17] Yang H., Liu H., Gao R., Liu X., Yu X. and Song F, Liu L. Numerical simulation of paint stripping on CFRP by pulsed laser. *Optics & Laser Technology* **145** (2022), 107450.

[18] Gao Q., Li Y., Wang H., Liu W., Shen H. and Zhan X. Effect of scanning speed with UV laser cleaning on adhesive bonding tensile properties of CFRP. *Applied Composite Materials* **26**(4) (2019), 1087-1099.

[19] Lu Y., Yang L., Wang M. and Wang Y. Improved thermal stress model and its application in ultraviolet nanosecond laser cleaning of paint. *Applied Optics* **59**(25) (2020), 7652-7659.

[20] Katnam K., Da Silva L. and Young T. Bonded repair of composite aircraft structures: A review of scientific challenges and opportunities. *Progress in Aerospace Sciences* **61** (2013), 26-42.

[21] Chen T., Wang W., Tao T., Pan A. and Mei X. Multi-scale micro-nano structures prepared by laser cleaning assisted laser ablation for broadband ultralow reflectivity silicon surfaces in ambient air. *Applied Surface Science* **509** (2020), 145182.

[22] Chillè C., Papadakis V. and Theodorakopoulos C. An analytical evaluation of Er:YAG laser cleaning tests on a nineteenth century varnished painting. *Microchemical Journal* **158** (2020), 105086.

[23] Bayle M., Waugh D.G., Colston B.J. and Lawrence J. On the study of oil paint adhesion on optically transparent glass: Conservation of reverse paintings on glass. *Applied Surface Science* **357**(Part A) (2015), 293-301.

[24] Li C.H., Ju X., Wu W.D., Zhu Q.H. and Zheng W.G. A universal theoretical model for thermal accumulation in materials during repetitive pulsed laser processing. *International Journal of Laser Science: Fundamentals Theory and Analytical Methods* **1**(1) (2018), 53-71.

[25] Li X., Wang D., Gao J., Zhang W., Li C., Wang N. and Lei Y. Influence of ns-laser cleaning parameters on the removal of the painted layer and selected properties of the base metal. *Materials (Basel)* **13**(23) (2020), 563.

[26] Li Z., Zhang D., Su X., Yang S., Xu J., Ma R., Shan D. and Guo B. Removal mechanism of surface cleaning on TA15 titanium alloy using nanosecond pulsed laser. *Optics & Laser Technology* **139** (2021), 106998.

[27] Yilmazer A. and Kocar C. Heat conduction in convectively cooled eccentric spherical annuli: A boundary integral moment method. *Thermal Science* **21**(5) (2017), 2255-2266.

[28] Qiu Y., Qiu X., Guo X., Wang D. and Sun L. Thermal analysis of Si/GaAs bonding wafers and mitigation strategies of the bonding stresses. *Advances in Materials Science and Engineering* **2017** (2017), 1-8.